AIAA-2000-1589

FLUTTER ANALYSIS OF THE X33

Samuel B. Fowler *
Structural Dynamic and Loads Group/ED21
NASA/Marshall Space Flight Center
Huntsville, AL 35812

ABSTRACT

Flutter analysis performed in support of the X33 Advanced Technology Demonstrator is described. Analysis was conducted over a range of flow regimes using several different analysis codes. The finite element and aerodynamic models used in the analysis have undergone several years of development and refinement resulting in a high degree of model detail. The flutter analysis focuses on the area of three critical points within the vehicle's design trajectory at which full sets of external loads have previously been developed. A comparison between several different aerodynamic models is also made for the selected trajectory points.

INTRODUCTION

During the past four years, the Structural Dynamics and Loads Group (ED21) of the Marshall Space Flight Center (MSFC) have been involved with the structural analysis and verification of the X33 (Fig. 1). In conjunction with industry partner Lockheed-Martin Corporation, NASA-MSFC has been tasked with the job of building and analyzing math models used to predict dynamic loads expected during flight.

As part of that effort, flutter analysis during atmospheric flight has been identified as one area requiring investigation. Given that the first portion of the X33's flight is in the lower atmosphere as a conventional aircraft, and that the X33 supports several lifting surfaces, the possibility of flutter occurring must be determined.

Initially, this analysis was undertaken with the purpose of serving as an independent verification on earlier flutter analysis work done by Lockheed-Martin. Although initial flutter analysis using earlier models had been done in the subsonic and supersonic regimes of flight, no flutter analysis using theory developed specifically for the transonic regime had been done. Hence, this area was targeted along with other subsonic and supersonic trajectory points since several critical values of the X33's design trajectory occur near this transonic area of flight. Additionally, the analysis scope was expanded in order to make use of the updated and revised finite element models of the X33 along with the different aerodynamic models available.

DESCRIPTION OF ANALYSIS

Two different software codes were used to obtain the aerodynamic influence coefficients needed for use in the flutter analysis. Separate codes were used due to the fact that differing flight regimes require different aerodynamic theory. A listing of the trajectory points analyzed along with the computational tools used is shown in Table 1 and is taken from Reference 1. MSC/NASTRAN was used for the subsonic and supersonic analysis. For subsonic analysis, the Doublet Lattice Method (DLM) aerodynamic code within MSC/NASTRAN was used. For supersonic analysis, the ZONA51 module from within MSC/NASTRAN was used. [2]

ZONA's ZTAIC6 code was used for the transonic aerodynamic analysis. Steady pressure data for the vehicle's lifting surfaces were interpolated from computational fluid dynamics (CFD) analyses via a FORTRAN program[3] and then interpolated onto the structural model using a newly developed approach which makes use of current computer aided engineering (CAE) software. (see Appendix A)

STRUCTURAL MODELING

The MSC/NASTRAN structural finite element model (FEM) of the X33 is currently in its sixth revision. A plot of the X33 structural dynamic model

* Aerospace Technologist, Structural Dynamics

is shown in Figure 2. Each revision has resulted in a complete loads cycle covering critical loading areas such as maximum dynamic pressure (MaxQ), transient lift-off, and prelaunch winds. The MSC/NASTRAN structural model exists as a loosely assembled set of bulk data include files with each file representing a portion of the model (i.e. port canted fin (CFIN), starboard vertical fin (VFIN), thrust assembly, LH2 tank, etc.). The model consists of over 50 MSC/NASTRAN bulk data files for a final assembled model of over 120,000 degrees of freedom. Loads from sources such as thrust, venting, and aerodynamic loads created from CFD are included into MSC/NASTRAN so that the full dynamic environment of load vectors affecting the vehicle is available for selected trajectory points.[4]

For all the flutter solutions, structural frequencies and modal vectors were obtained by eigenvalue solution for a selectively chosen reduced set of nodes (ASET) from within MSC/NASTRAN.[5] For the MSC/NASTRAN solutions, a full model representation was used. For the ZONA/ZTAIC6 solutions, a half model excluding the body flap nodes within the ASET was used. Tables 2 and 3 contain a listing of the modes selected for inclusion in the analysis for both the MSC/NASTRAN and ZONA cases. The modes selected for inclusion were based on overall structural motion that could influence flutter with certain isolated local modes being eliminated from study. It is noted that the MSC/NASTRAN cases were run with a model that was one revision more current than the ZONA cases. During this revision, mass was added to the model in several places resulting in an overall lowering of some fundamental frequencies. A FORTRAN program provided from ZONA was used to write the MSC/NASTRAN data into a form that ZONA/ZTAIC6 could recognize.

Separate aerodynamic models were created for use in ZONA and in MSC/NASTRAN. The original MSC/NASTRAN aerodynamic model was created for ED21 under contract and was used in a previous static aeroelastic analysis of the X33 vehicle. It is in its second revision[6] and is referred to as Configuration TZ. It treats the fins and fuselage as lifting surfaces with some geometric allowances made for endplating of the canted fins into the body, and is shown in Figure 3. It consists of 454 lifting surface elements. The second MSC/NASTRAN aerodynamic model was created by Lockheed-Martin and represents the entire vehicle as a lifting surface. It consists of a finer mesh than the previous configuration (TZ) as it contains 2020 lifting surface elements. This model is referred to as Configuration LM and is shown in Figure 4. For the sake of comparison, the LM model's canted fin surface mesh is approximately seven times finer that of the TZ model and takes about 7 times as much CPU time to obtain a solution.

The ZONA/ZTAIC6 aerodynamic model is a symmetric half model generated from within the ZONA code. For this model, the canted and vertical fins are treated as lifting surfaces that require steady pressure input. The body is represented as such with a constant steady input. The model is shown in Figure 5.

RESULTS

Structural frequency and damping plots for the selected Mach number and different aerodynamic model cases are shown in Figures 6-11 and 13-14. As would be expected, the modes primarily involved with the non-lifting surface areas such as global vehicle yaw, pitch, and bending modes show virtually no aeroelastic coupling effect for any of the selected Mach numbers.

Generally speaking, the .78 (Fig. 6 and 7) and .84 (Fig. 9 and 10) cases show more of an aeroelastic effect than the 1.3 (Fig. 13 and 14) case. Additionally, the LM aerodynamic model configuration (Figs. 7, 10, and 14) shows more aeroelastic effect than the TZ aerodynamic model configuration (Figs. 6, 9, and 13) for elastic modes that include lifting surface areas such as CFIN bending and torsion. This is to be expected since the LM configuration has a much finer mesh as mentioned previously. It is noted that no thickness correction factors were used for the M=1.3 case (Figs. 13 and 14). Use of a thickness correction factor has been shown to provide more realistic results in the supersonic flight regime.[2]

Some modal crossovers at speeds greater than 1.15 V_d are noted to occur such as between modes 14/15 and 16/17 on Figure 10. However, these modes occur in different areas of the vehicle (CFIN/VFIN) and would not tend to influence one another greatly. Generally speaking, no modal crossovers were observed to occur at less than 1.15 V_d for all analyzed cases.

Observing the damping plots provides little more information than that found in the frequency-velocity plots. For Figure 13, a couple of modes (31,34,40) have slightly positive damping values in the lower velocity ranges that do not diverge. Typically, damping traces of the non-lifting surface areas are the least negative but prove to be the most stable over the velocity range for the MSC/NASTRAN cases. Note that mode 42 on Figure 13 does show an erratic oscillation in damping response which corresponds to its frequency trace as well. Structural dampings for the ZONA/ZTAIC6 cases (Figs. 8 and 11) are suspect across the entire velocity range and are included only for completeness.

Figure 12 is included as a comparison between the linear (subsonic) and nonlinear (transonic) theory solutions available in ZONA/ZTAIC6 for the M= .84 case. Note that for this case, the linear solution is approximately the same as the nonlinear solution out to about 800 Keas.

CONCLUSIONS

The overall assessment of Figures 6-14 across the various models and methods described in this analysis indicate that the X33 is free of flutter for the trajectory points studied.

The LM aerodynamic model configuration seems to be more sensitive than the TZ aerodynamic model. This in itself is not surprising since the TZ model is much coarser and was meant primarily for static aeroelastic analysis. However, comparison and study of the two models yields some insight into how one single model might be built in the future for use with static and dynamic aeroelastic analyses.

The use of the ZONA/ZTAIC6 transonic method, which incorporates actual steady pressures from either experiment or CFD, can be tedious for large FEM models although the process was carried through in this analysis. As shown in Figure 12, it appears that there is no quantifiable reason to use the nonlinear solution for this particular case. Additional cases in the transonic region (particularly closer to Mach 1) would need to be evaluated for any final assessment of when to use the nonlinear method or when to know if the linear method would provide reasonable results. The results obtained from the nonlinear solution remain somewhat suspect in this analysis due to the inconsistent damping results. Factors such as the lack of iteration control inherent in the K method, the use of an incomplete, earlier FEM model, and CFD interpolation/approximation may have introduced some error into the final results.

SUMMARY

Flutter analysis for the X33 vehicle has been carried out using the most current finite element models available. The analysis made use of several different codes and flutter methods while examining three different flight regimes over the vehicle's trajectory. A CAE procedure for getting CFD steady pressure data over to nodal pressures that are usable in a finite element model was also developed. The analysis showed the X33 to be unaffected by flutter within the boundaries covered by this analysis.

ACKNOWLEDGEMENTS

Dave McGhee and Jeff Peck have done extensive work in the finite element modeling of the X33 vehicle. Alan Droege provided the CFD analysis used by the ZONA/ZTAIC6 code. Dr. Tom Zeiler of the University of Alabama put together the initial MSC/NASTRAN aerodynamic model of the X33. Thomas H. Walsh and R. Shane Weatherwax put together the Lockheed-Martin aerodynamic model of the X33. Darius Sarhaddi and P.C. Chen provided helpful guidance with the ZONA/ZTAIC6 code.

REFERENCES

1. Structural Design Criteria and Design Loads (604D0011) of the X-33 Advanced Technology Demonstrator, Revision E, May 1998, (Proprietary Data).

2. Rodden, W.P. and Johnson, E.H., "MSC/NASTRAN Aeroelastic Analysis", Version 68, The MacNeal-Schwendler Corporation, 1994.

3. Documentation of ZTAIC6 Code, ZONA Technology (Proprietary), March 1996.

4. McGhee, D.S, "A Strategy for Integrating a Large Finite Element Model Using MSC NASTRAN/PATRAN: X-33 Lessons Learned", NASA TM-1999-209201.

5. Reymond, Michael, and Miller, Mark, "MSC/NASTRAN Quick Reference Guide", Version 69, The MacNeal-Schwendler Corporation, 1996.

6. Zeiler, Thomas A. and Gomeringer, Timothy, "Static Aeroelastic Modeling and Analysis in Support of X-33 Development", NASA H-30025D Final Report, April 1999.

Mach #	CFD Description	Regime	Vd (Keas)	Trajectory Point	Flutter Solution/Code
0.78	α=-4.0°,Q=342	Subsonic	365	MaxQ (51402), Malmstrom, 25k @ 58 s	MSC/NASTRAN Doublet Lattice-PK method
0.78	α=-4.0°,Q=342	Subsonic	365	MaxQ (51402), Malmstrom, 25k @ 58 s	ZONA/ZTAIC6 Linear K Method
0.84	α=5.5°,Q=342	Subsonic	391	MaxQ (51401), Malmstrom, 25k @ 58 s	MSC/NASTRAN Doublet Lattice-PK method
0.84	α=5.5°,Q=342	Subsonic	391	MaxQ (51401), Malmstrom, 25k @ 58 s	ZONA/ZTAIC6 Linear – K Method
0.84	α=5.5°,Q=342	Transonic	391	MaxQ (51401), Malmstrom, 25k @ 58 s	ZONA/ZTAIC6 Nonlinear – K Method
1.3	α=5.5°,Q=319	Supersonic	355	MaxQ (52401), Malmstrom, 48.5k @ 86 s	MSC/NASTRAN ZONA51 – PK Method

Table 1 – Chart of Trajectory Points.

Mode	Frequency (Hz)	Description
1	1.535	Global pitching mode
2	1.940	Global yawing mode (mainly aeroshell)
3	5.049	CFIN 1st Bending (Asymmetric)
4	5.142	CFIN 1st Bending (Symmetric)
5	7.494	Body Flaps 1st Bending (mainly port)
6	7.534	Body Flaps 1st Bending (mainly starboard)
7	8.716	Pitch Mode/Bending about y-axis (mainly nose)
8	8.797	Very similar to #7
9	9.842	Global yawing mode
10	10.244	Yawing mode of nose
11	11.611	VFIN 1st Bending/Nose pitching
14	14.617	CFIN Flap Bending (Asymmetric)
15	14.664	CFIN Flap Bending (Symmetric)
16	14.982	VFIN 1st Bending (Symmetric)
17	14.988	VFIN 1st Bending (Asymmetric)
18	15.494	CFIN 1st Torsion (Symmetric)
19	16.529	CFIN 1st Torsion (Asymmetric)
26	20.342	Slight CFIN Aileron Torsion (Symmetric)
27	20.426	Slight CFIN Aileron Torsion (Asymmetric)
30	22.359	CFIN 2nd Bending (Asymmetric)/VFIN Torsion
31	22.546	VFIN 1st Torsion (Asymmetric)
32	22.655	VFIN 1st Torsion (Symmetric)
33	22.745	CFIN 2nd Bending (Symmetric/VFIN Torsion)
34	23.006	CFIN 2nd Bending (Asymmetric)
40	26.197	Slight CFIN Torsion (Asymmetric)
42	27.701	Slight CFIN 2nd Bending

Table 2 – Frequencies/Mode Shapes for Subsonic/Supersonic (MSC/NASTRAN) Cases.

Mode	Frequency (Hz)	Description
0-6	0.000	Rigid Body Modes
7	5.597	Vehicle & CFIN bending, VFIN torsion
8	6.610	CFIN 1st Bending
9	7.975	Vehicle 2nd Bending
12	14.907	CFIN 2nd Bending, VFIN 1st Bending
13	15.833	VFIN 1st Bending, CFIN flap motion
14	16.813	CFIN 1st Torsion, slight VFIN bending
15	17.123	CFIN & VFIN Torsion, Vehicle bending
16	19.161	VFIN & Vehicle Bending (slight)
21	22.219	Vehicle Bending, Ruddervator torsion
22	22.749	VFIN 2nd Bending /Torsion, Vehicle bending
26	25.710	CFIN 2nd Bending
27	26.018	Vehicle Torsion/Bending
34	34.012	VFIN Torsion
37	36.693	VFIN Torsion
39	43.218	CFIN 3rd Bending

Table 3 – Frequencies/Mode Shapes for Transonic (ZONA/ZTAIC6) Cases.

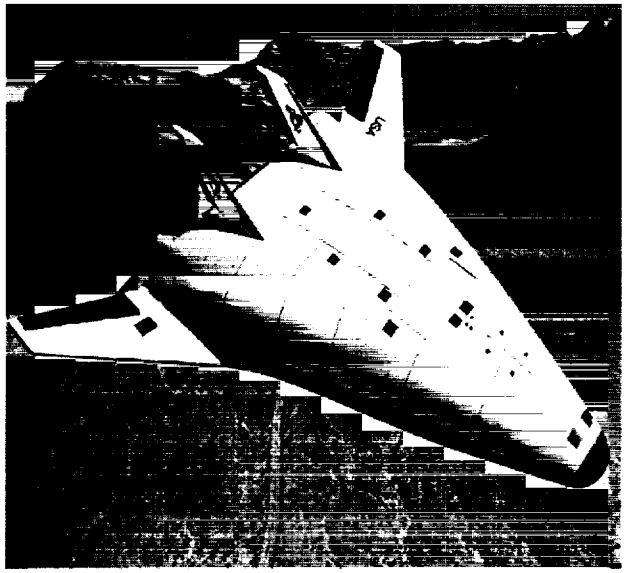

Figure 1. X33 Advanced Technology Demonstrator.

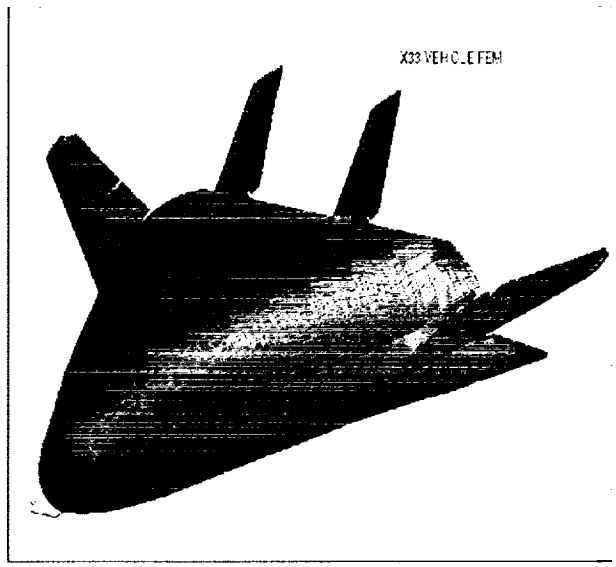

Figure 2. MSC/NASTRAN FEM of X33.

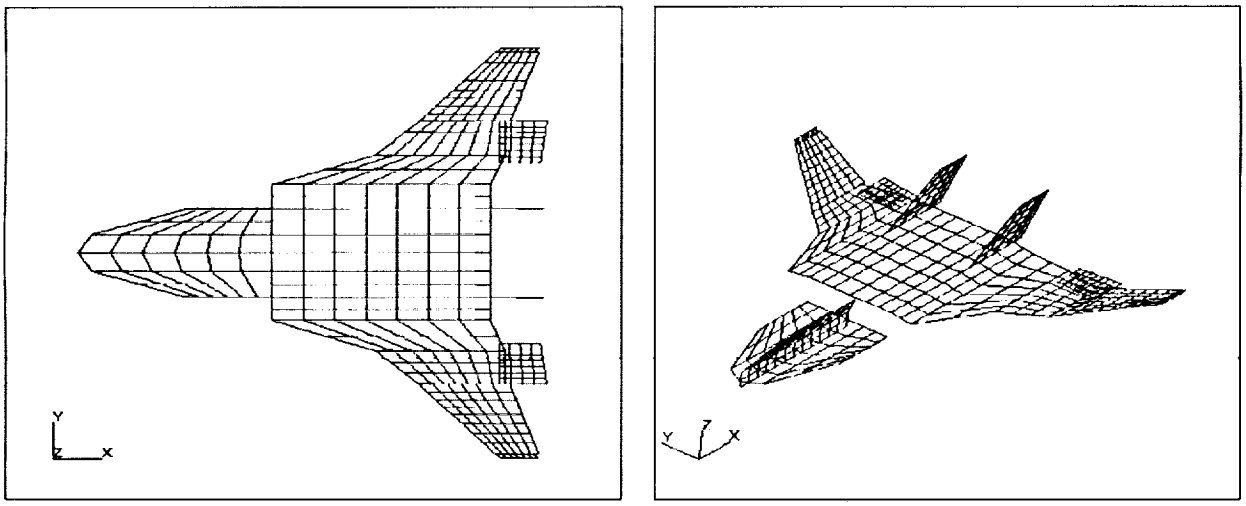

Figure 3. TZ Configuration MSC/NASTRAN Aerodynamic Model of X33.

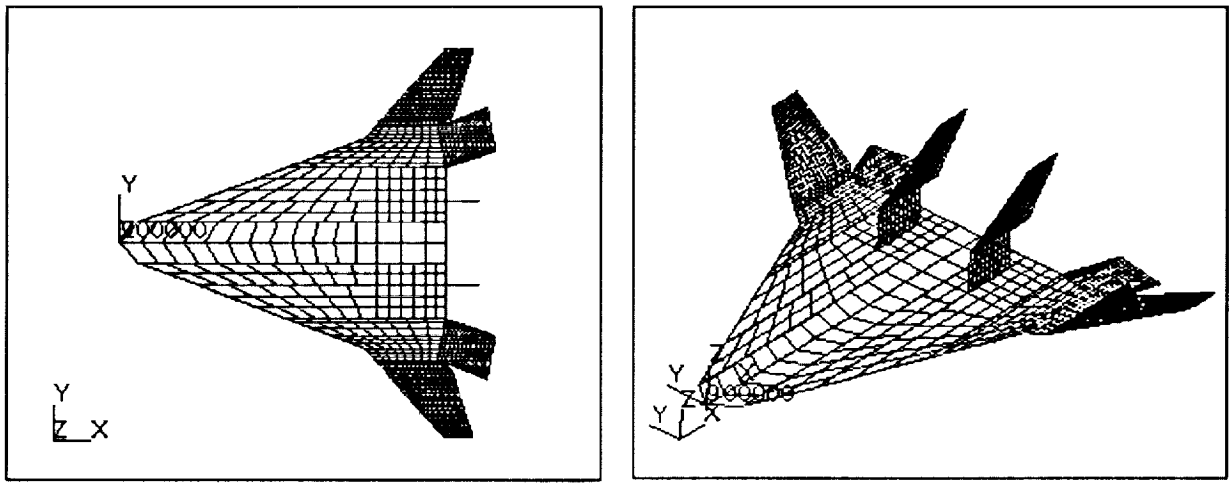

Figure 4. LM Configuration MSC/NASTRAN Aerodynamic Model of X33.

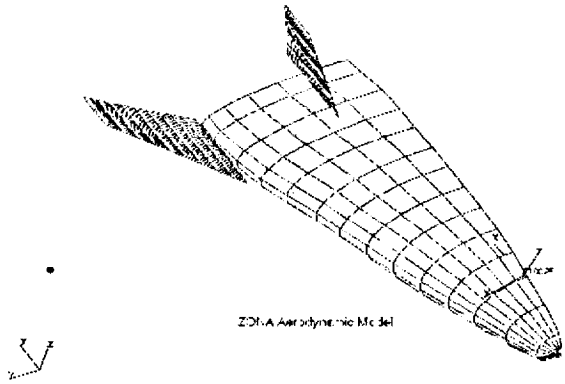

Figure 5. ZONA/ZTAIC6 Aerodynamic Model of X33.

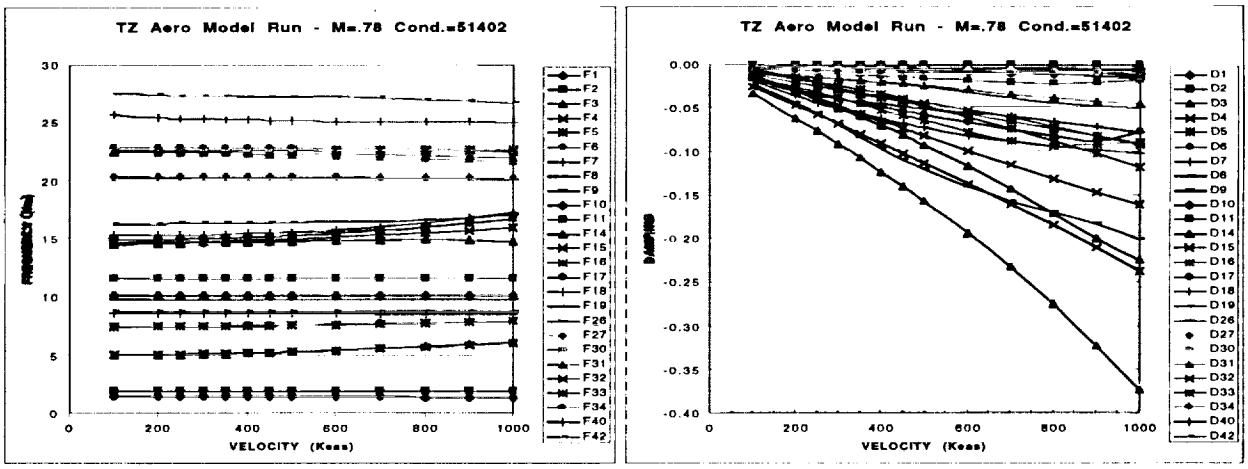

Figure 6. Frequency/Damping Plots For M=0.78, TZ Configuration.

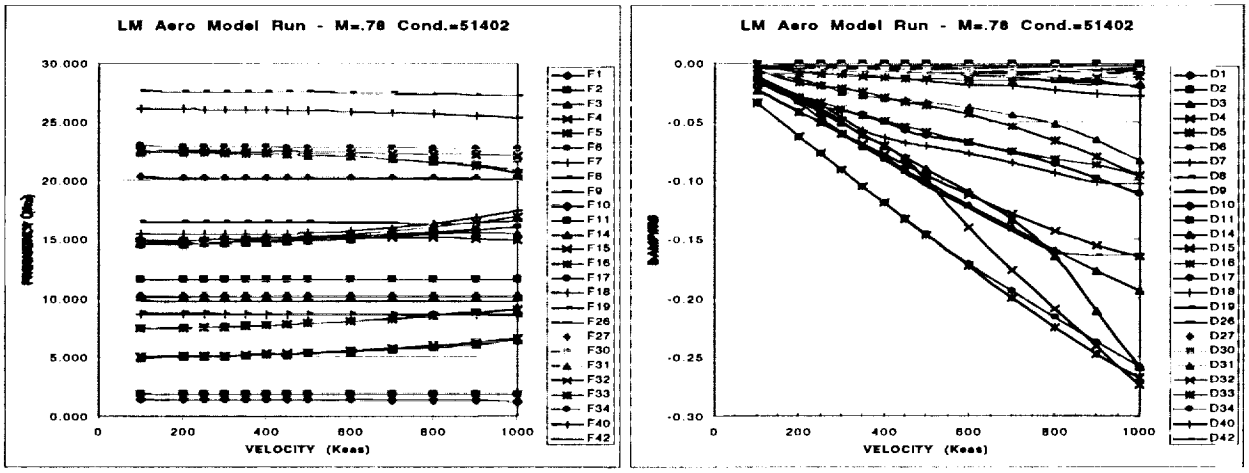

Figure 7. Frequency/Damping Plots for M=0.78, LM Configuration.

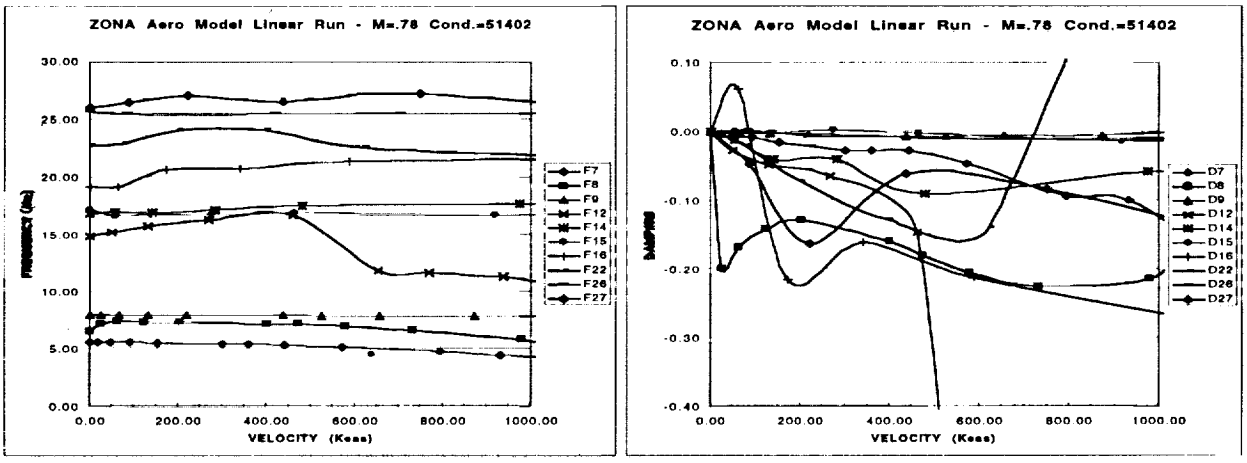

Figure 8. Frequency/Damping Plots for M=0.78, ZONA-Linear Solution.

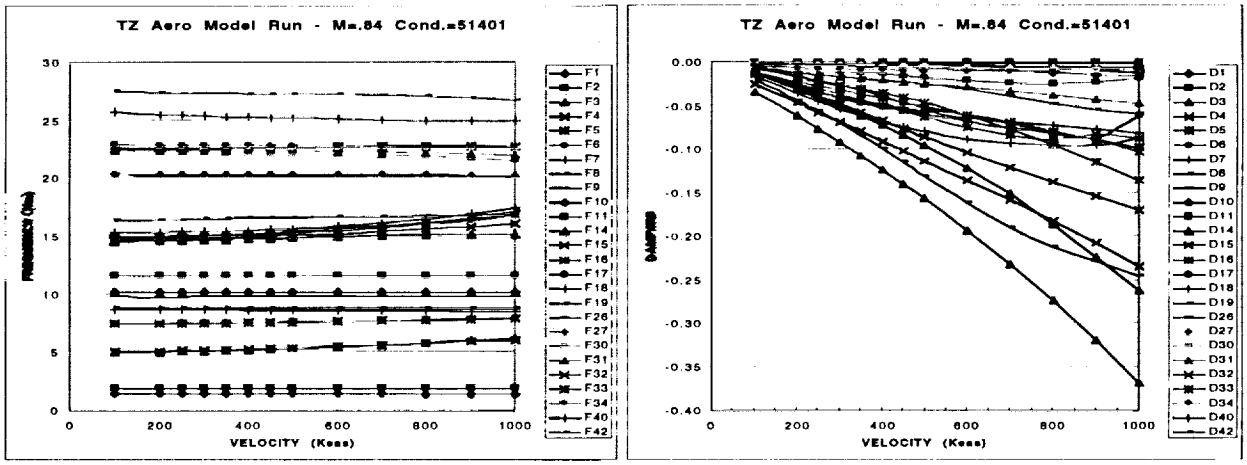

Figure 9. Frequency/Damping Plots for M=0.84, TZ Configuration.

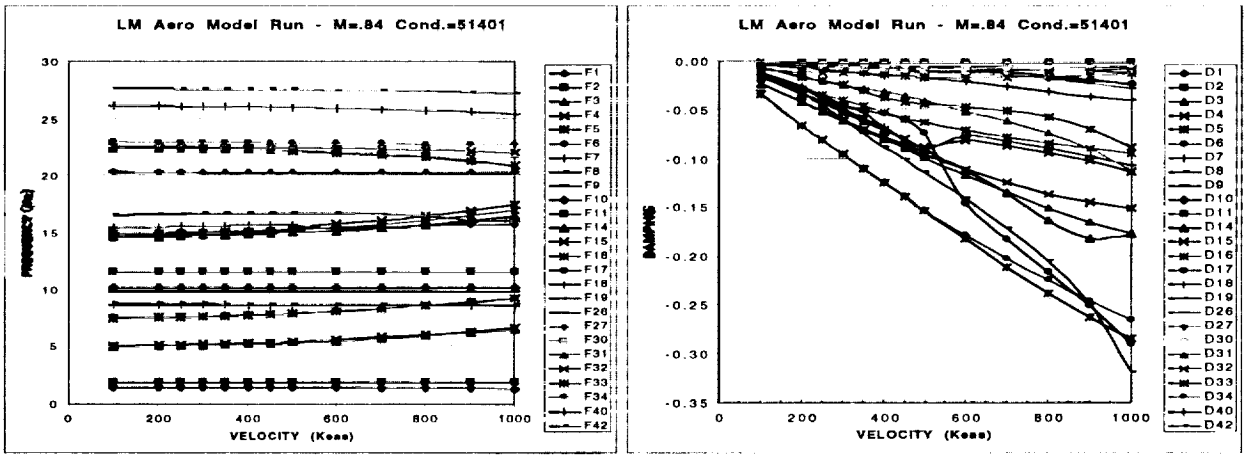

Figure 10. Frequency/Damping Plots for M=0.84, LM Configuration.

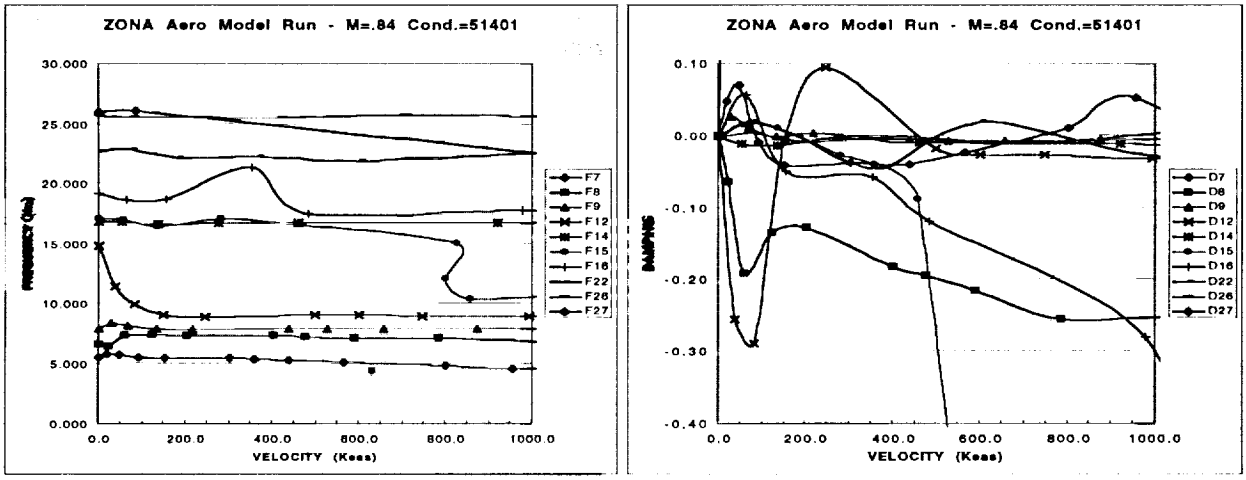

Figure 11. Frequency/Damping Plots for M=0.84, ZONA/ZTAIC6-NonLinear Solution.

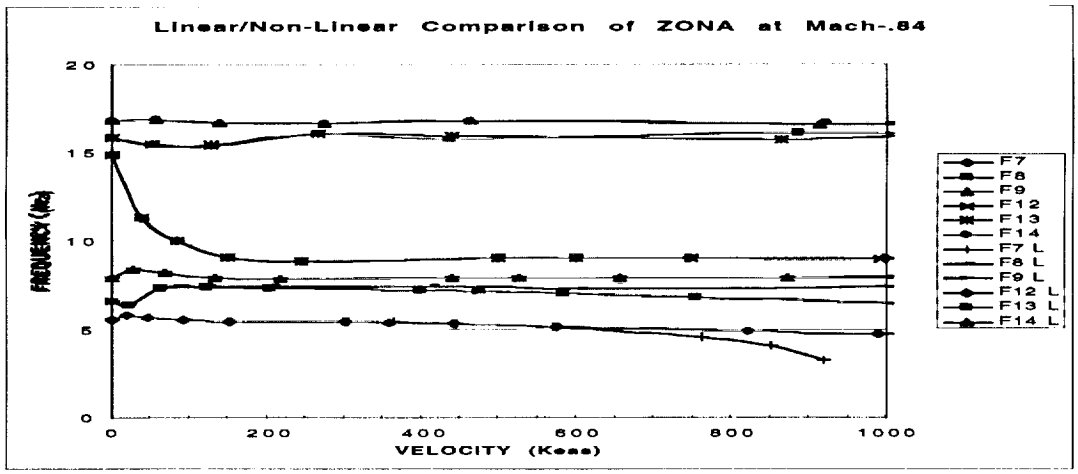

Figure 12. Comparison of Linear/Non-Linear ZONA/ZTAIC6 Solutions at M=0.84.

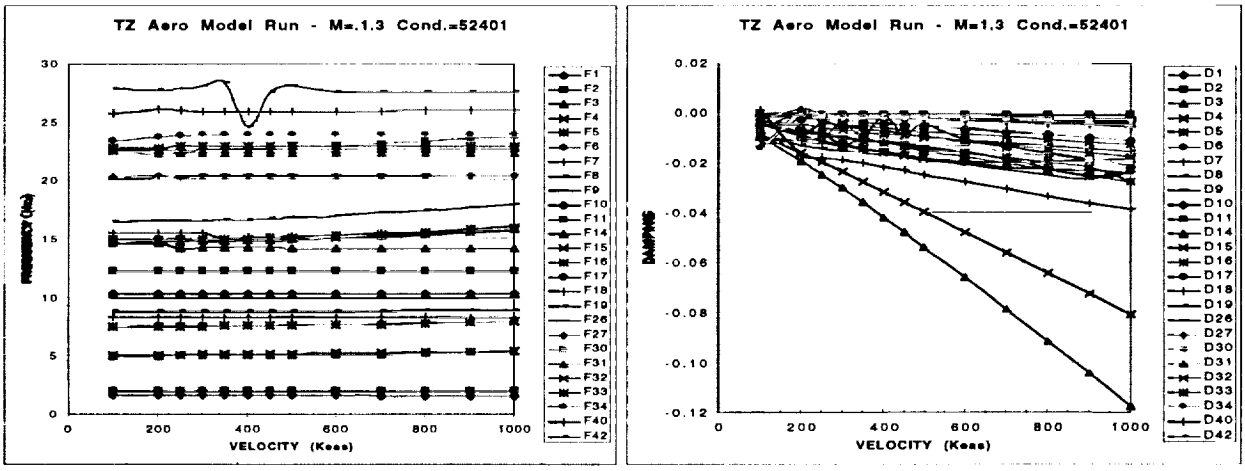

Figure 13. Frequency/Damping Plots for M=1.3, TZ Configuration.

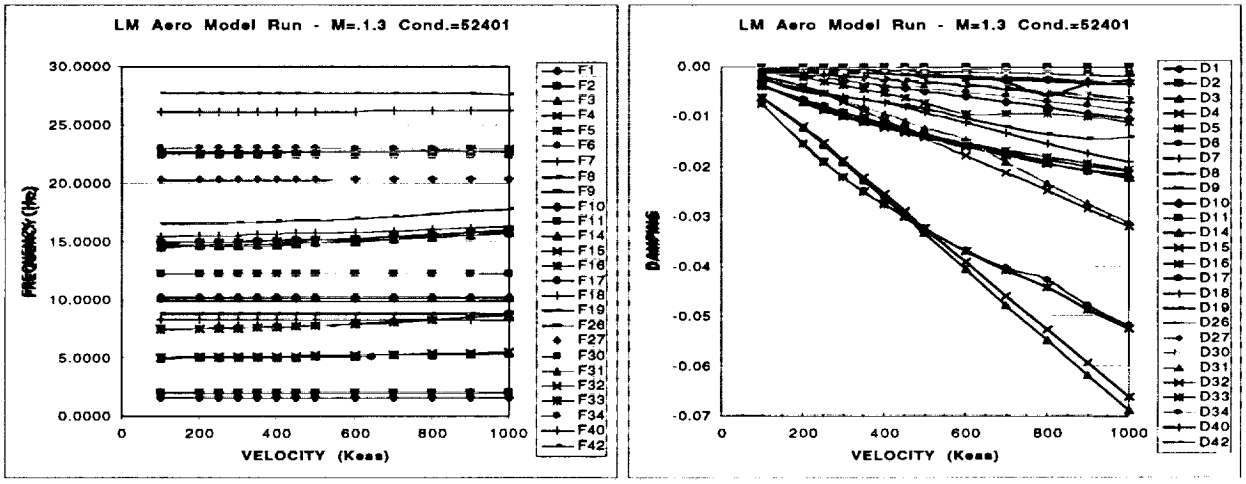

Figure 14. Frequency/Damping Plots for M=1.3, LM Configuration.

APPENDIX A

CFD to FEM Interpolation

Steady pressure data were input to the ZONA/ZTAIC6 deck by means of manipulating FEM loads data obtained from interpolated CFD results. This process combines several steps inside of the CAE software PATRAN along with a FORTRAN program that interpolates from a CFD mesh to a structural mesh. The process of interpolating the CFD data to a FEM mesh, selecting geometric dimensions on the upper and lower surfaces of the lifting surfaces, and reducing this data to chordwise and spanwise locations is the most labor intensive and error prone portion of the analysis.

Figures A1 and A2 show the FEM mesh surface of interpolated pressures after running the FORTRAN program. Within the figures, the individual chordwise lines in the upper and lower surfaces can be seen. These lines have to be determined parallel to the flow and coplanar with the surface and may be created using features found within PATRAN.

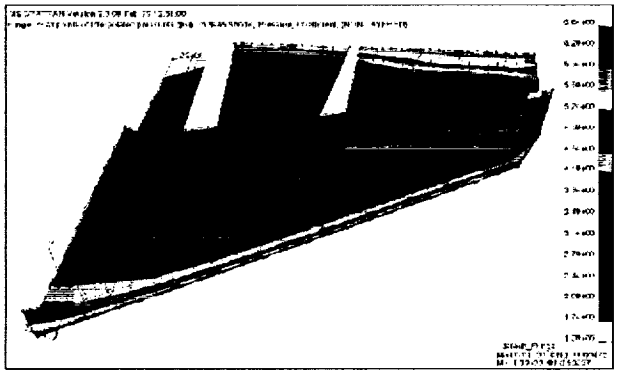

Figure A1. Interpolated CFD-FEM Pressure for Outer Chord Line of Upper Surface on CFIN.

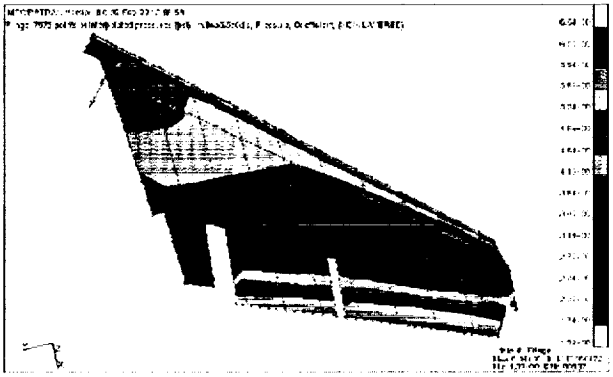

Figure A2. Interpolated CFD-FEM Pressure for Outer Chord Line of Lower Surface on CFIN.

Figures A3 and A4 show the chordwise pressure coefficient values used for each span for the upper and lower canted fin surfaces in the ZONA/ZTAIC6 transonic solution. The values are obtained by interpolating the FEM pressure data within PATRAN to the individual chord lines. This procedure of CFD interpolation to FEM degrees of freedom is performed in a like manner for the vertical fin. Additionally, one can see that although changing other parameters such as angle of attack and Mach number to run different trajectory points is accomplished rather easily, each distinctive case requires an iteration of the interpolation procedure described above to obtain unique unsteady pressures within the transonic range. Hence, only one trajectory point in the transonic area was chosen for this analysis.

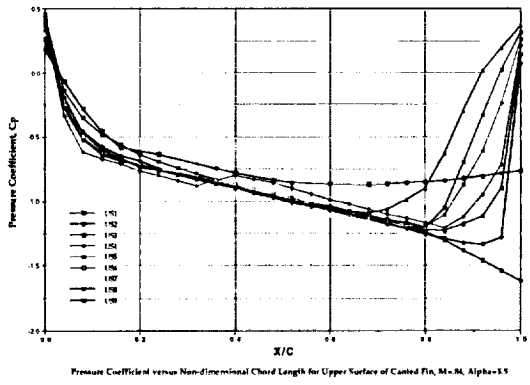

Figure A3. Upper Surface Spanwise Interpolated Pressure Coefficients for CFIN.

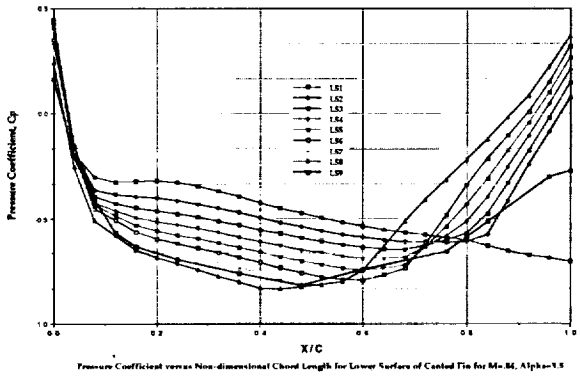

Figure A4. Lower Surface Spanwise Interpolated Pressure Coefficients for CFIN.